BMC Genomics

RESEARCH

Open Access

Transcriptomic and proteomic profiling of piroplasmosis resistance in Yunnan humped cattle

Yuming Chen[1,2†], Xiaona Chen[1,3†], Rong Liu[1,2], Chunqing Li[1], Heng Xiao[1] and Shanyuan Chen[1*]

Abstract

Background Piroplasmosis, including Theileriosis and Babesiosis, poses a threat to livestock health and productivity worldwide. However, the molecular mechanisms underlying breed-specific differences in resistance to piroplasmosis remain poorly understood. Compared to *Bos taurus*, *Bos indicus* generally exhibits greater resistance to diseases such as piroplasmosis and trypanosomiasis, as well as enhanced adaptability to hot and humid environments. Yunnan humped cattle, an indigenous *B. indicus* breed, are well adapted to coarse feed and harsh environments, yet the molecular basis of their disease resistance has not been systematically investigated.

Results By integrating transcriptomic and proteomic analyses, we demonstrated that genetic background is the primary determinant shaping distinct immune response strategies between cattle breeds. Mucosal immunity and innate immunity emerged as key contributors to differential resistance to piroplasmosis. We identified several candidate genes and protein biomarkers highly expressed in Yunnan humped cattle, including *CCL4*, *CCL5*, *IL1R2*, *IL5RA*, *BOLA*, *BOLA-DRB3*, *IFNB1*, and the protein HPX. These candidates are likely to be directly or indirectly involved in host resistance to piroplasmosis and may have potential utility as molecular markers.

Conclusions This study improves our understanding of disease resistance in Yunnan humped cattle. The identified candidate genes and proteins may serve as molecular markers for marker-assisted breeding, offering a theoretical basis for developing cattle populations resistant to piroplasmosis.

Keywords Yunnan humped cattle, Simmental cattle, Piroplasmosis, Transcriptome, Proteome

†Yuming Chen and Xiaona Chen contributed equally to this work.

*Correspondence:
Shanyuan Chen
chensy@ynu.edu.cn
[1]School of Ecology and Environmental Science, Yunnan University, Kunming 650500, China
[2]State Key Laboratory for Conservation and Utilization of Bio-Resources in Yunnan, Yunnan University, Kunming 650091, China
[3]School of Medical Technology, Yunnan Medical Health College, Kunming 650032, China

Background

Piroplasmosis, including theileriosis and babesiosis, is caused by protozoan parasites that infect the blood of both domesticated and wild animals. These parasites pose a serious threat to livestock health and productivity and are also considered animal-derived zoonotic pathogens [1, 2]. Piroplasmosis is primarily transmitted by ticks [3, 4], and its occurrence has been reported in many provinces of China [5, 6]. Therefore, identifying effective strategies to control and mitigate the impact of this parasitic disease is of great importance.

Cattle are one of the earliest domesticated breeds and play an important role in the meat, dairy, and leather industries [7]. However, the large scale and density of farming increase the risk of disease outbreaks and pathogen transmission. In the absence of sufficient host immunity, reliance on external drug treatments alone may facilitate pathogen proliferation [8]. An alternative and sustainable approach is to exploit inherent host resistance and parasite tolerance through genetic improvement and selective breeding for disease resistance [9–12]. Taurine cattle (*Bos Taurus*) and zebu cattle (*Bos Indicus*) represent the two major domesticated cattle lineages worldwide. Compared with taurine cattle, zebu cattle generally exhibit stronger resistance to diseases, as well as better tolerance to heat and humidity [13, 14]. Notable differences have been reported between these two cattle types in resistance to trypanosomosis, tick infestation, and piroplasmosis [15–20]. Yunnan humped cattle are an indigenous zebu breed in China and share the typical characteristics of *B. indicus* [14]. In contrast, Simmental cattle are a widely farmed taurine cattle breed. In this study, Yunnan humped cattle and Simmental cattle were selected to compare their resistance to piroplasmosis, to provide a theoretical basis for reducing the impact of this disease.

RNA sequencing (RNA-seq) is a high-throughput technology widely used to analyze transcriptome composition and gene expression levels in cells and tissues [21]. It can be used to study various traits and find the genetic basis of differences [16]. In proteomics, mass spectrometry (MS)-based quantitative approaches mainly include data-dependent acquisition (DDA) and data-independent acquisition (DIA) [22]. DIA has the advantages of panoramic scanning and data traceability, which can overcome several limitations of the traditional DDA method [23, 24], and has been successfully applied in clinical research and biomarker discovery [25–28].

In this study, piroplasmosis was investigated as a broad parasitic disease entity through a preliminary integrative transcriptomic and proteomic analysis to explore the genetic basis of resistance in Yunnan humped cattle. This integrative approach characterizes host responses at the disease-group level, providing an overall perspective on piroplasmosis in cattle. Our objectives were to elucidate differences in disease resistance between Yunnan humped and Simmental cattle and to identify molecular markers and functional pathways associated with resistance. These findings provide a valuable foundation for further exploration of the unique traits of the Yunnan humped cattle, an important indigenous breed.

Methods

Sample collection and preparation

In this study, whole blood, plasma, and serum samples were collected from 30 Yunnan Humped cattle and 12 Simmental cattle in Lancang County, Pu'er City (Yunnan, China), and from 45 Yunnan humped cattle and 31 Simmental cattle from Mangshi City, Dehong Prefecture (Yunnan, China) (Additional file 1).

Genomic DNA was extracted from whole blood samples using the Tiangen DNA extraction kit (DP304; Tiangen Biotech, Beijing, China). PCR amplification was performed to detect the presence of piroplasm DNA using primers reported in previous studies [29, 30], with detailed primer information provided in Additional file 2. Sample grouping was primarily based on PCR detection results.

Microscopic examination of Giemsa-stained blood smears was performed as a supplementary method to visually assess the presence of piroplasm. Briefly, a drop of fresh anticoagulated blood was spread into a thin smear, air-dried, fixed with methanol, and stained with diluted Giemsa solution (stock solution: deionized water = 1:10) for 15–30 min. Slides were gently rinsed with water and examined under an OLYMPUS BX50 light microscope (Olympus, Tokyo, Japan). Due to the asymptomatic or carrier status of the animals and the associated low parasitemia, blood smear examination was not used as the primary criterion for group classification.

PCR assays were used to detect piroplasm infections, including *Babesia* spp. and *Theileria* spp. For this study, animals positive for either genus were collectively classified as piroplasmosis-positive and analyzed together. Based on PCR results, Yunnan humped cattle positive for piroplasms were assigned to the Zebu experimental group (Z-EG), and PCR-negative individuals to the Zebu control group (Z-CG). Similarly, PCR-positive Simmental cattle were classified as the Simmental experimental group (X-EG), and PCR-negative individuals as the Simmental control group (X-CG). A total of 118 animals were initially sampled to assess piroplasmosis prevalence. For transcriptomic and proteomic analyses, a subset of animals was selected based on PCR-confirmed infection status to define experimental and control groups for downstream analyses. In Lancang, 15 Yunnan humped cattle (5 Z-EG and 10 Z-CG) and 10 Simmental cattle (5 X-EG and 5 X-CG) were selected. In Mangshi, 20 Yunnan

humped cattle (10 Z-EG and 10 Z-CG) and 14 Simmental cattle (4 X-EG and 10 X-CG) were included for subsequent analyses. Because piroplasm infection status could only be determined by PCR after sample collection, and all animals were clinically asymptomatic, equal group sizes could not be predefined.

RNA extraction and library construction and RNA sequencing

Above 59 blood samples were used for transcriptomic analysis. RNA sequencing was performed by Majorbio Bio-Pharm Technology Co., Ltd. (Shanghai, China), following standardized protocols. Total RNA was extracted from whole blood using TRIzol reagent (Invitrogen, Carlsbad, CA, USA). The quantity and purity of total RNA were detected by the NanoDrop ND-2000 C spectrophotometer (Thermo Fisher Scientific, Waltham, MA, USA). Furthermore, RNA integrity was detected by Agilent 2100 Bioanalyzer (Agilent Technologies, Santa Clara, CA, USA). RNA libraries were constructed using the Illumina TruSeq™ mRNA Sample Preparation Kit (Illumina, San Diego, CA, USA). Briefly, mRNA was enriched using oligo(dT) magnetic beads, fragmented, and reverse-transcribed into cDNA. Approximately 300 bp fragments were selected using magnetic beads and ligated to sequencing adapters. Libraries were amplified by 15 cycles of PCR, and target fragments were recovered using 2% agarose gel electrophoresis. Library concentrations were quantified using a TBS380 fluorometer with PicoGreen reagent, and libraries were pooled equimolarly. Cluster generation was performed by bridge PCR amplification on a cBot system, followed by paired-end sequencing (2 × 150 bp) on an Illumina NovaSeq 6000 platform [31] (Illumina, San Diego, CA, USA). On average, approximately 44–55 million raw reads were generated per sample.

Transcriptome analysis of DEGs

Raw data quality was assessed using FastQC (Version: 0.11.9), and quality reports were integrated with MultiQC [32] (Version: 1.6). Adapter sequences and low-quality bases (Phred score < 20) were removed using Trim Galore (v0.6.7). After quality control, each sample retained more than 43 million clean reads, with an overall mapping rate of > 92% and a unique mapping rate of > 88%. Clean reads were aligned to the *Bos taurus* reference genome (ARS-UCD1.2) using HISAT2 [33] (Version: 2.2.1) software, with the corresponding GTF annotation file. Gene expression levels were quantified as transcripts per million (TPM). Differential expression analysis was performed using DESeq2 [34], and genes with $p < 0.05$ and $|\log_2 \text{fold change}| > 1$ were defined as differentially expressed genes (DEGs). To minimize the confounding effect of inherent breed differences, DEGs identified in the piroplasm-negative comparison (Z-CG vs. X-CG) were excluded from subsequent infection-related breed comparisons. This strategy aimed to highlight infection-associated, breed-specific molecular responses rather than baseline genetic differences between breeds. The DEGs obtained from Z-EG vs. X-EG formed a gene set called EG_unique, and these genes were used for functional enrichment analysis.

Protein extraction, digestion, and DIA-based proteomic analysis

We chose plasma samples consistent with the above 25 individuals from Lancang, and 19 individuals from Mangshi (5 Z-EG and 5 Z-CG, 4 X-EG and 5 X-CG) for proteomic analysis. Protein extraction, digestion, and DIA analysis were performed by Majorbio Bio-Pharm Technology Co., Ltd. (Shanghai, China), following standardized protocols.

High-abundance plasma proteins were depleted using the ProteoMiner™ Protein Enrichment Kit (Bio-Rad Laboratories, Hercules, CA, USA). Protein concentration was then measured, and quality control was performed. The protein solution was dissolved and enzymatically digested to prepare peptide samples. Pooled peptide samples were analyzed in data-dependent acquisition (DDA) mode to generate a spectral library, while individual samples were analyzed in data-independent acquisition (DIA) mode for quantitative proteomic profiling. Mass spectrometry (MS) analysis was performed using an Orbitrap Astral mass spectrometer (Thermo Fisher Scientific, Bremen, Germany). Equal amounts of peptides were dissolved in MS buffer, and 10x indexed retention time (iRT) peptides were added before MS analysis.

DIA data processing and protein identification

DDA raw files were searched using Proteome Discoverer™ v.2.4 [35] to construct the spectral library. Protein identification was performed against a combined UniProt database including *Bos taurus* (UP000009136) and *Bos indicus* (UP000515132). Then the protein was subsequently imported into Spectronaut software [36] for DIA data analysis. The iRT peptides were used for retention time calibration. Protein-level and peptide-level FDR were both controlled at ≤ 1%, and peptide identification confidence was set to ≥ 99%. The extracted ion chromatogram (XIC) extraction window was set to 75 ppm. The non-linear regression of iRT peptides showed that the majority of data points were evenly distributed along the fitted curve, indicating stable retention time alignment and good chromatographic performance across samples. Protein intensities were normalized based on total peak area and used for downstream quantitative analysis. For DIA-based protein quantification, up to six peptides per

protein were selected, and for each peptide, three fragment ions were used for quantitative analysis.

Proteomic analysis of DEPs

Protein quantification was based on DIA intensities extracted by Spectronaut. Differential protein expression analysis was performed on proteins passing the above identification criteria. Due to the relatively limited sample size and the conservative nature of FDR correction in DIA-based proteomic data, differential protein expression was initially screened using Student's t-test with a nominal $p < 0.05$ and fold change ≥ 1.2 or ≤ 0.83. This approach was adopted for the exploratory identification of candidate differentially expressed proteins (DEPs). False discovery rates (FDRs) were calculated for all quantified proteins; however, due to the limited number of proteins passing stringent FDR thresholds in plasma DIA data, nominal p-values combined with fold-change criteria were applied to retain biologically relevant candidates for downstream analyses. After removing the intersection proteins with Z-CG vs. X-CG, the differential proteins obtained from Z-EG vs. X-EG of Lancang samples and Mangshi samples formed protein sets called Z-EG vs. X-EG specific differential proteins, and then these proteins were used for functional enrichment analysis.

Functional enrichment and protein–protein interaction network analyses

Functional enrichment analysis was carried out using Gene Ontology (GO) and Kyoto Encyclopedia of Genes and Genome (KEGG) analysis. GO and KEGG enrichment analyses were performed using the clusterProfiler package in R. For functional enrichment analysis, GO enrichment typically yields a large number of terms, which were evaluated using Benjamini-Hochberg adjusted p-values (p-adjust < 0.05). In contrast, KEGG pathway enrichment resulted in a relatively limited number of pathways; therefore, nominal p-values ($p < 0.05$) were used as a screening threshold to retain biologically interpretable pathways. Given the limited number of identified DEPs and enriched terms, nominal p-values ($p < 0.05$) were used as a screening threshold to identify potentially relevant biological functions and pathways.

Protein–protein interaction (PPI) networks were constructed to further explore key DEGs and DEPs. Genes and proteins associated with immunity and disease resistance were selected based on differential expression and functional annotation. Protein interactions between genes or proteins were analyzed based on the STRING database (https://cn.string-db.org/). The resulting file of genes obtained from the STRING database was downloaded and imported into Cytoscape software (v3.9.1) to plot and calculate the node degree of each gene to judge the importance.

Verification of DEGs and DEPs

To verify the transcriptomic data, we selected 8 DEGs from the Lancang samples and 9 DEGs from the Mangshi samples to do RT-qPCR experiments. RT-qPCR assays were performed by a commercial service provider, Majorbio Bio-Pharm Technology Co., Ltd. (Shanghai, China), following standardized protocols. According to the data provided by ICG [37], *GAPDH* was selected as the reference gene for RT-qPCR. After concentration and quality evaluation, the total RNAs were reverse transcribed to cDNA. ChamQ SYBR Color qPCR Master Mix (Vazyme Biotech Co., Ltd., Nanjing, China) and ABI QuantStudio 6 Real-Time PCR System (Applied Biosystems, Foster City, CA, USA) were used to do the RT-qPCR experiment. RT-qPCR was performed using a unified cycling program for all samples: initial denaturation at 95 ℃ for 5 min, followed by 35 cycles of denaturation at 95 ℃ for 30 s, annealing at 55 ℃ for 30 s, and extension at 72 ℃ for 1 min. The primers were provided by Shanghai Sangon Biological Engineering Co., Ltd. (Shanghai, China). The details of primers of RT-qPCR are shown in Additional file 2. Primer specificity was confirmed by amplification and melting curve analyses, showing a single specific peak. Primer efficiencies were validated by the service provider in accordance with MIQE guidelines.

To verify the protein expression and the expression trend, parallel reaction monitoring (PRM) [38, 39] was employed to quantify selected DEPs. PRM analysis was performed by a commercial service provider, Majorbio Bio-Pharm Technology Co., Ltd. (Shanghai, China), following standardized protocols. Peptide samples were prepared by reduction, alkylation, and enzymatic digestion, followed by analysis on an Orbitrap mass spectrometry platform in FULL MS-PRM acquisition mode with positive ion detection. Targeted peptide signals were extracted and quantified using Skyline software [40], and the peak areas of the fragment ions corresponding to the target protein were integrated. Stable-isotope-labeled internal standard peptides were not used; therefore, PRM quantification was performed in a label-free, relative manner. PRM results were used to assess the consistency of expression trends between targeted validation and global proteomic profiling.

Results

Piroplasm carriage rate varies across regions and cattle breeds

In samples collected from Lancang County, the piroplasm carrying rate was 16.67% (5/30) in Yunnan humped cattle and 58.33% (7/12) in Simmental cattle. Conversely, in Mangshi City, the carriage rate was 48.89% (22/45) in Yunnan humped cattle and 19.35% (6/31) in Simmental cattle (Fig. 1). Details of the PCR results of the piroplasm-positive Yunnan humped cattle are provided

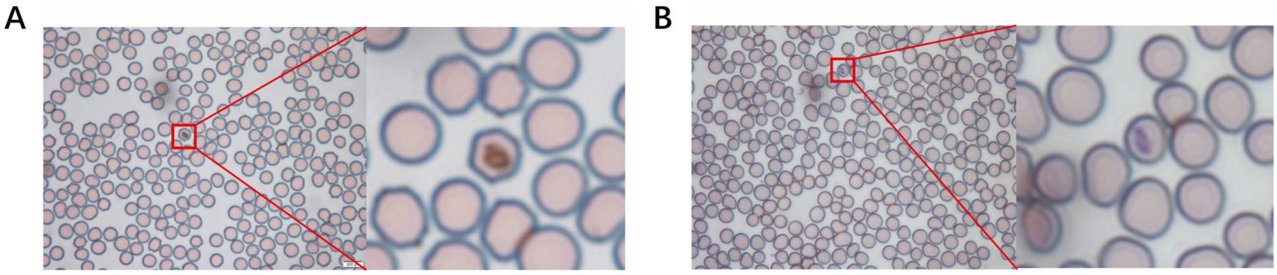

Fig. 1 Representative microscopic images of blood smears from cattle infected with piroplasm. Giemsa-stained thin blood smears showing the presence of piroplasm in red blood cells from (**A**) Yunnan humped cattle (sample Z10) and (**B**) Simmental cattle (sample X15). Blood smears were prepared from fresh anticoagulated blood, fixed with methanol, and stained with diluted Giemsa solution. Images were acquired using an OLYMPUS BX50 light microscope. Scale bars, 200 μm

in Additional file 3. To further explore the molecular differences, we performed principal component analysis (PCA) and heatmap clustering based on RNA-seq and DIA-based proteomic data (Fig. 2; Additional file 4). These analyses revealed clear separations between Yunnan humped and Simmental cattle, whereas piroplasm-positive and -negative individuals within the same breed showed minimal differences.

Transcriptome and proteome differences associated with cattle breed and piroplasm infection

After quality control of the transcriptomic data, a total of 18,397 genes and 63,168 transcripts were obtained in Lancang samples, while 27,152 genes and 91,840 transcripts were detected in the Mangshi samples. Summary statistics of the sequencing data are presented in Additional file 5. Using the criteria of $p < 0.05$ and $|\log2FC| > 1$, 1,382 differentially expressed genes (DEGs) were identified in the Z-EG vs. X-EG comparison in Lancang samples, and 968 DEGs were identified in Mangshi samples. In the Z-CG vs. X-CG comparison, 1713 DEGs were detected in Lancang samples, and 1204 DEGs in Mangshi samples (Fig. 3). These results indicate extensive transcriptional differences between Yunnan humped and Simmental cattle that are consistent across both regions.

In proteomics analysis, DIA-based mass spectrometry of plasma samples shows that the percentage of identified peaks exceeded 64% in all groups, indicating that the spectral library was appropriate and the results were reliable (Additional file 5). DEPs were identified using the criteria of $FC \geq 1.20$ for upregulated proteins, $FC \leq 0.83$ for downregulated proteins, and $p<0.05$. In the Lancang samples, 96 DEPs were identified in the Z-EG vs. X-EG comparison and 154 DEPs in the Z-CG vs. X-CG comparison. In the Mangshi samples, 52 DEPs were identified in Z-EG vs. X-EG and 64 DEPs in Z-CG vs. X-CG (Fig. 4).

To specifically investigate the genes and proteins expressed associated with piroplasmosis, we focused on the piroplasm-positive groups (Z-EG vs. X-EG) while excluding the DEGs and DEPs identified in the piroplasm-negative comparison (Z-CG vs. X-CG). Using this approach, we obtained 491 DEGs and 33 DEPs from the Lancang samples, and 637 DEGs and 36 DEPs from the Mangshi samples for subsequent analysis (Fig. 5). This approach effectively minimized breed-specific background effects unrelated to parasite carriage, allowing us to focus on infection-associated molecular signatures. These infection-associated DEGs and DEPs were further analyzed to explore their potential biological functions.

Immune-related functional enrichment of differentially expressed genes and proteins

To gain insight into the biological functions of the DEGs, Gene Ontology (GO) and KEGG enrichment analyses were conducted. In the GO analysis, 491 DEGs identified from the Lancang samples were significantly enriched in 13 GO terms ($p < 0.05$) (Fig. 6A; Additional file 6). Notably, several terms, such as antimicrobial humoral immune response mediated by antimicrobial peptides, innate immune response in mucosa, and mucosal immune response, were related to host immune defense and disease resistance. Similarly, the 637 DEGs from the Mangshi samples were significantly enriched in 25 GO terms (Fig. 6B; Additional file 6). Enriched terms such as immune response, negative regulation of viral genome replication, and defense response to symbiont further supported the involvement of immune-related biological processes.

In the proteomic GO enrichment analysis of the Lancang samples, only four differentially expressed proteins (DEPs) were enriched in two GO terms. Specifically, A0A140T851 and Q9BGI3 were associated with glandular development (GO:0048732), while A0A6P5C9U8 and P00921 were enriched in lysozyme activity (GO:0016829). Notably, among Mangshi samples, 21 DEPs were enriched in 30 GO terms ($p < 0.05$) (Fig. 6C; Additional file 6). Several of these terms were immune-related, including: innate immune response of mucosa, organ or tissue-specific immune response, mucosal immune response, regulation of interferon γ-mediated signaling pathway, and regulation of γ-interferon response. Among the enriched proteins, F1N3Q7 and F1MLW2 proteins

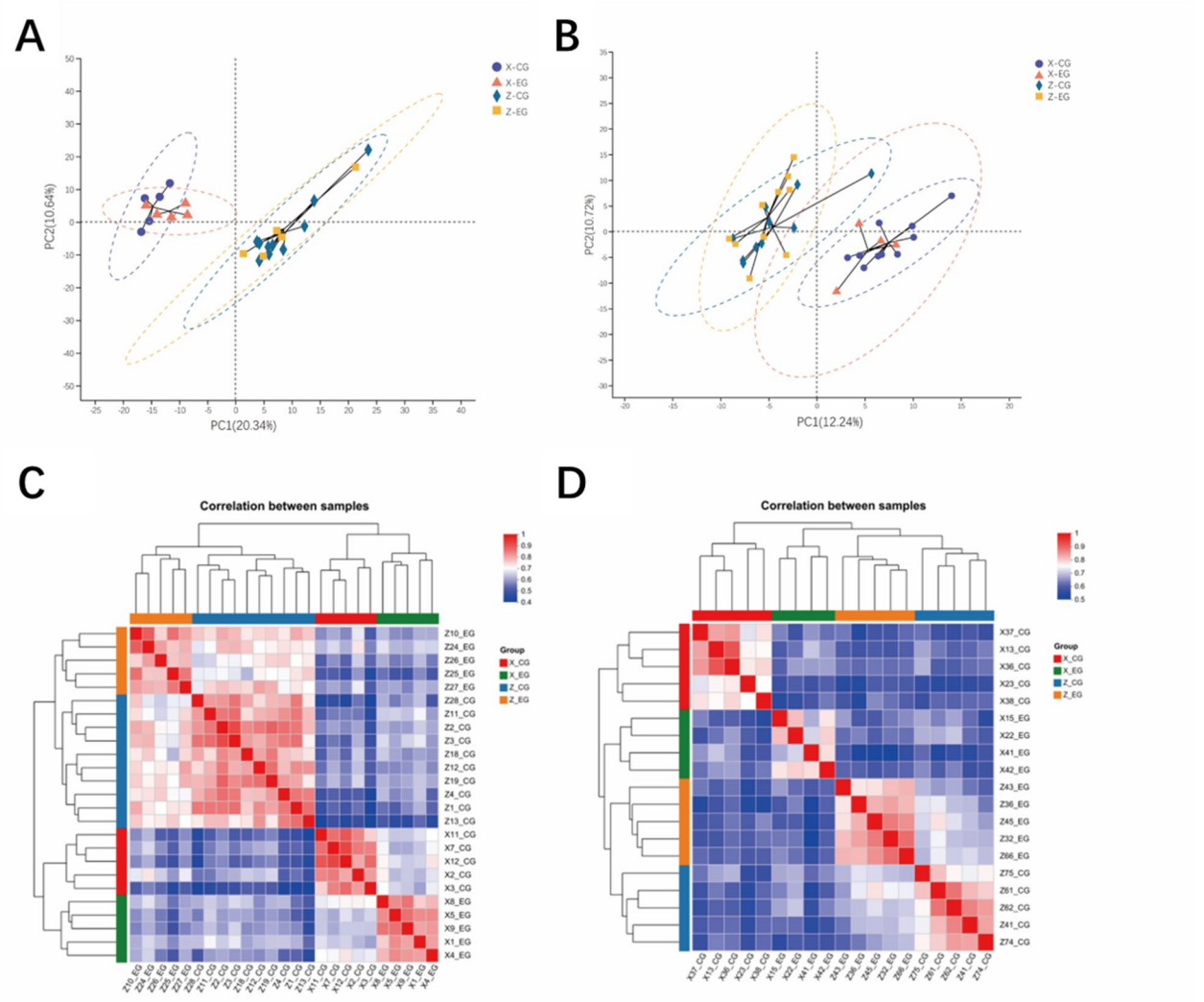

Fig. 2 Correlation analysis of samples from Lancang and Mangshi. The PCA analysis based on normalized transcriptome data of Lancang (**A**) and Mangshi (**B**) samples. Heatmaps show Pearson correlation coefficients between samples based on proteome data from Lancang (**C**) and Mangshi (**D**). Different colors in the heatmaps represent the magnitude of the correlation coefficient, with higher absolute values indicating stronger correlations

were involved in mucosal innate immune responses and tissue-specific immune regulation. These findings were consistent with the transcriptomic enrichment results, suggesting that innate and mucosal immunity may contribute to the differential resistance to piroplasmosis observed between Yunnan humped cattle and Simmental cattle.

In order to further elucidate functional differences between Yunnan humped cattle and Simmental cattle in the piroplasm-positive groups (Z-EG vs. X-EG), KEGG pathway enrichment was also performed. In the Lancang samples, 491 DEGs were significantly enriched in 17 KEGG pathways ($p < 0.05$) (Fig. 7A; Additional file 6). Among these, several pathways annotated as immune or disease-related were identified, including neutrophil extracellular trap formation, Staphylococcus aureus infection, and malaria. Although systemic lupus erythematosus and rheumatoid arthritis were also enriched, these terms likely reflect general inflammatory activation rather than disease-specific autoimmune processes in cattle. In the Mangshi samples, 637 DEGs were enriched in 66 pathways (Fig. 7B; Additional file 6), of which 35 pathways were associated with immunity, infectious disease, and signal transduction. Notable pathways included intestinal immune network for IgA production, leishmaniasis, African trypanosomiasis, natural killer cell-mediated cytotoxicity, and the B cell receptor signaling pathway.

In terms of differential proteins, there were no significant pathways enriched in Lancang-specific differential proteins (L-SDPs), but 8 pathways were significantly enriched in 36 Mangshi-specific differential proteins

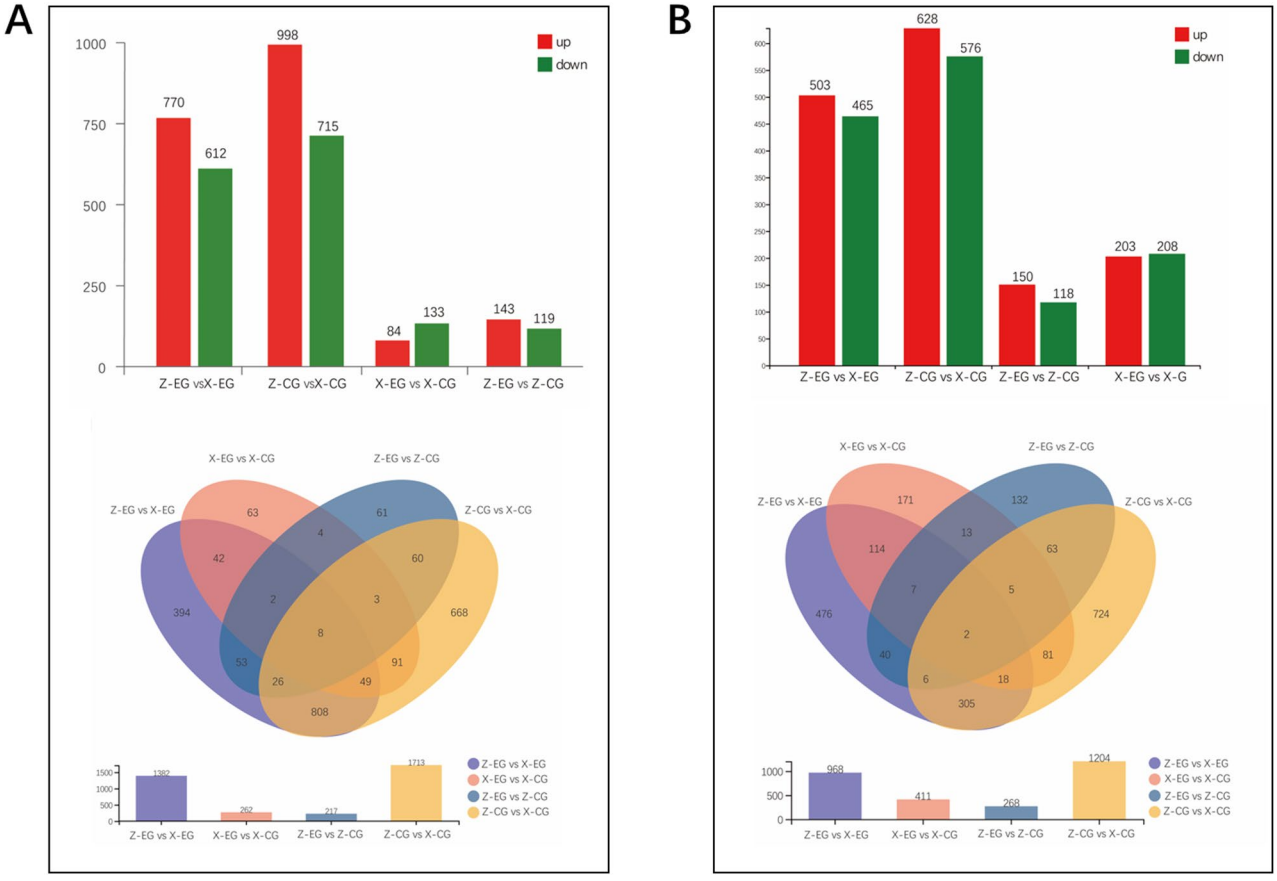

Fig. 3 Bar plot and Venn plot of significantly differentially expressed genes (DEGs). DEGs were identified using DESeq2, with genes showing $p < 0.05$ and |log2FC| > 1 considered significant. Bar plots show the number of upregulated (red) and downregulated (green) genes, and Venn diagrams display shared and specific DEGs among different groups. **A** DEGs in Lancang samples. **B** DEGs in Mangshi samples

(M-SDPs), including some immune and disease-related pathways, such as the TGF-β signaling pathway, Salmonella infection, hepatitis B, and PI3K-Akt signaling pathway (Fig. 7C; Additional file 6). In summary, these enrichment results revealed significant transcriptional and proteomic differences between the two cattle breeds in immune-related processes, particularly those involving innate and mucosal immunity. Subsequent analyses, therefore, focused on key genes and proteins within these enriched pathways to further clarify their potential roles in piroplasmosis resistance.

Protein–protein interaction networks of DEGs and DEPs for identification of key candidate genes and proteins

To further explore the molecular basis of immune and disease resistance differences between Yunnan humped cattle and Simmental cattle, we integrated DEG expression levels with GO and KEGG enrichment results. Based on this, 117 genes from the Lancang samples and 197 genes from the Mangshi samples were selected for protein–protein interaction (PPI) network construction. Analysis of the PPI networks revealed several hub genes potentially involved in the differential resistance to piroplasmosis (Fig. 8). In the Lancang samples, the top 10 weighted hub genes are mainly related to immune response, inflammation, and immune system regulation. In Mangshi samples, the top 20 key hub genes are involved in anti-bacterial and anti-virus immunity.

To identify the most relevant candidate genes, stringent selection criteria were applied, including a fold change ≥ 4, adjusted $p < 0.05$, enrichment in immune- or parasite-related GO terms and KEGG pathways, localization as nodes within the PPI network, and known associations with immunity or disease. As a result, we identified 7 genes in the Lancang samples (*SRC*, *TNFSF11*, *CCL4*, *BOLA-DRB3*, *LOC281376*, *FCAR*, *IL1R2*) and 11 genes in the Mangshi samples (*CCL5*, *IFNB1*, *THBS1*, *LOC100297725*, *NKG2C*, *BOLA*, *IL5RA*, *CD1A*, *P2RX7*, *TNFRSF12A*, *TNFRSF9*), which were relatively highly expressed in the Yunnan humped cattle (Additional file 7).

Similarly, to investigate the interactions among key DEPs and to identify hub proteins, GO and KEGG enrichment results were integrated to select immunity-,

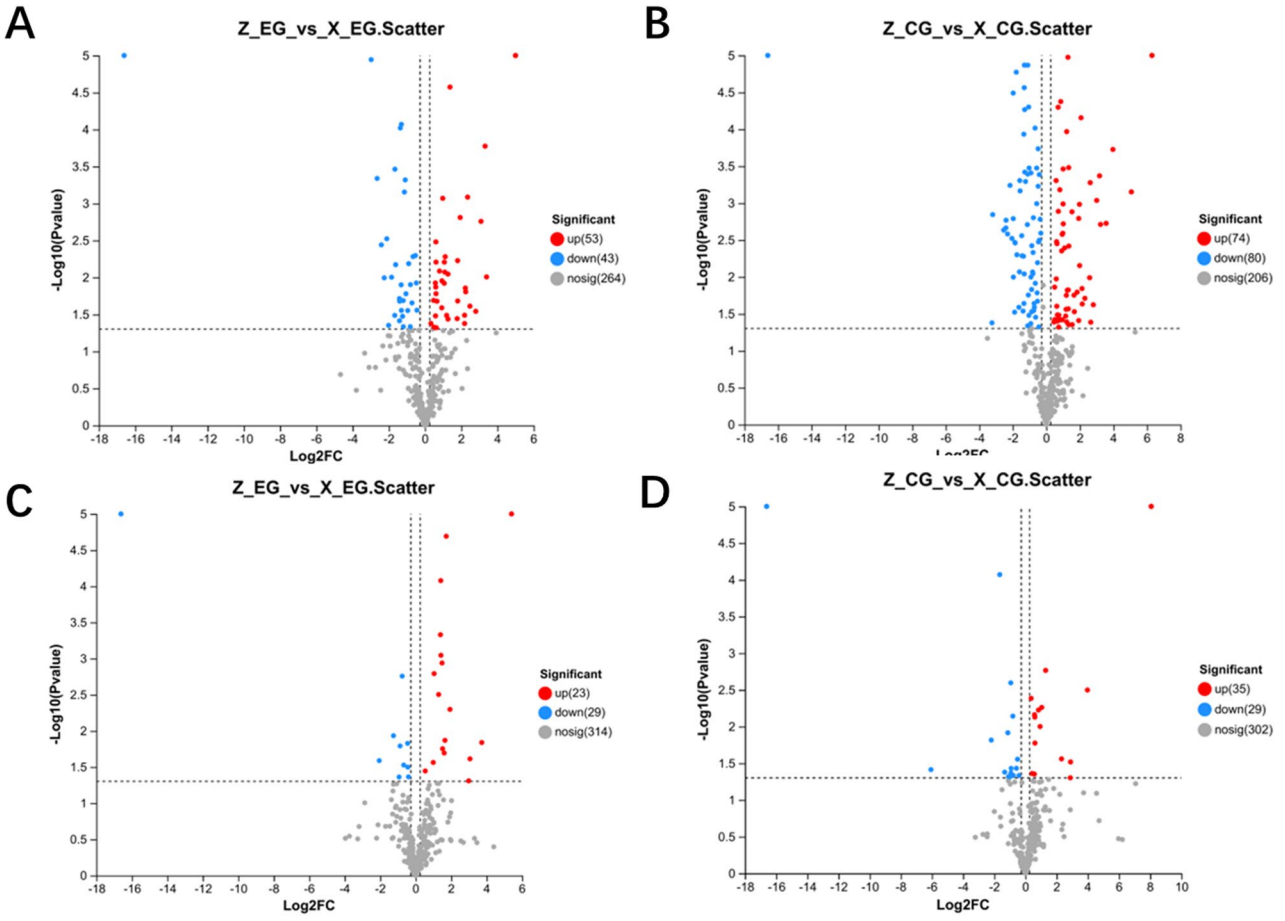

Fig. 4 Volcano map of differentially expressed proteins (DEPs). Each dot represents one protein. Proteins with $p < 0.05$ were considered significant. Red and blue dots indicate upregulated and downregulated proteins, respectively. **A** DEPs of Z-EG vs. X-EG group in Lancang samples. **B** DEPs of Z-CG vs. X-CG group in Lancang samples. **C** DEPs of Z-EG vs. X-EG group in Mangshi samples. **D** DEPs of Z-CG vs. X-CG group in Mangshi samples

inflammation-, and disease-related DEPs from the Mangshi samples (Additional file 8) for PPI analysis. We selected 12 proteins to construct a PPI network to identify the candidate proteins (Fig. 9). According to the PPI network, HPX (Hemopexin isoform X1) and APOA4 (Apolipoprotein A4) showed a moderate interaction (combined score = 0.648), whereas the interaction between HPX and LUM (Lumican) was relatively weak. However, interaction between FMOD (Fibromodulin) and LUM is the strongest, with a composite score of 0.954 (Additional file 8). Based on protein expression levels, the HPX protein is significantly highly expressed in Yunnan humped cattle, suggesting that it has potential as a protein biomarker associated with piroplasmosis resistance in Yunnan humped cattle.

Verification of DEGs and DEPs

To validate the transcriptomic data, 8 (3 up, 5 down) and 9 (2 up, 7 down) randomly selected DEGs were analyzed by RT-qPCR. The expression levels detected by RT-qPCR for all genes matched well with the transcriptome data, demonstrating that the RNA-seq results in this study are reliable (Fig. 10). To assess the reliability of DIA-based proteomic quantification, we employed the PRM technique to perform relative quantification of selected DEPs. The PRM validation was conducted using plasma samples from the same Z-EG and X-EG groups in the Mangshi samples. Three representative DEPs were selected for PRM analysis based on their significant differential expression identified by DIA analysis ($p < 0.05$). PRM results confirmed that these proteins exhibited expression trends consistent with those observed in the DIA-based proteomic data (Fig. 11; Additional file 8).

Discussion

B. indicus has adapted to hot and humid environments for a long time, which leads to different disease resistance from *B. taurus* [41, 42]. By integrating transcriptomic and proteomic analyses with bioinformatics approaches, this study provides initial insights into the molecular basis underlying the differential resistance to piroplasmosis between Yunnan humped cattle and Simmental cattle.

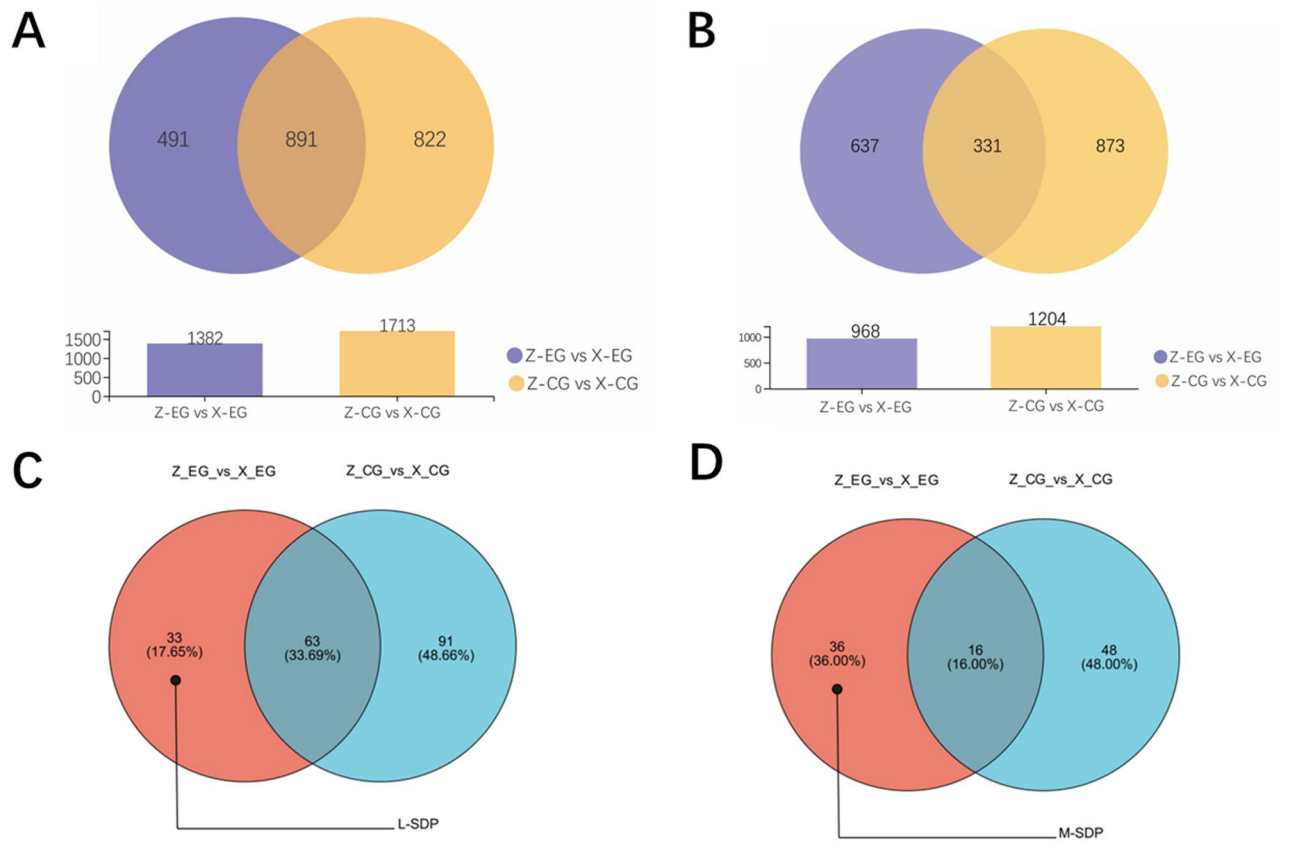

Fig. 5 Venn diagram of DEGs and DEPs of the Z-EG vs. Z-CG comparison. Genes and proteins were identified using the same criteria as described in Figs. 3 and 4. **A** Venn diagram and statistical chart of DEGs in the Lancang sample. **B** Venn diagram and statistical chart of DEGs in the Mangshi sample. **C** Venn diagram of DEPs in the Lancang sample, where the specific differentially expressed proteins are defined as L-SDPs. **D** Venn diagram of DEPs in the Mangshi sample, where the specific differentially expressed proteins are defined as M-SDPs

Our research further elucidates the genetic basis underlying the characteristics of Yunnan humped cattle, highlighting the potential mechanisms for their resistance to piroplasmosis.

Genetic background contributes to divergent immune response strategies

Our results indicate that both host genetic background and environmental factors, such as regional parasite diversity and ecological conditions, may jointly shape infection dynamics. In Lancang County, the piroplasm carrying rate among Simmental cattle (58.33%) was significantly higher than that among Yunnan humped cattle (16.67%), whereas in Mangshi, the opposite trend was observed. This suggests that responses to piroplasm infection differ between cattle breeds in a context-dependent manner and may be influenced by region-specific factors, including parasite strain composition, vector distribution, climatic conditions, and husbandry practices. PCA analysis revealed substantial differences in transcriptomic and proteomic profiles between the two breeds, whereas infection status accounted for relatively smaller variation within each breed (Fig. 2). This suggests that breed-related genetic background represents an important contributor to immune response patterns, while environmental and infection-related factors may further modulate these responses.

Mucosal immunity and innate immunity represent key differences in piroplasmosis resistance between two cattle breeds

After eliminating breed-specific background effects, we conducted functional enrichment analysis of DEGs and DEPs identified in the piroplasm-positive groups. We acknowledge that this filtering strategy may also remove infection-relevant genes that are shared by both breeds. However, our primary objective was to identify molecular features underlying differential infection responses between breeds rather than common host responses to piroplasmosis. The transcriptomic data from both Lancang and Mangshi samples showed significant enrichment in GO terms related to mucosal and innate

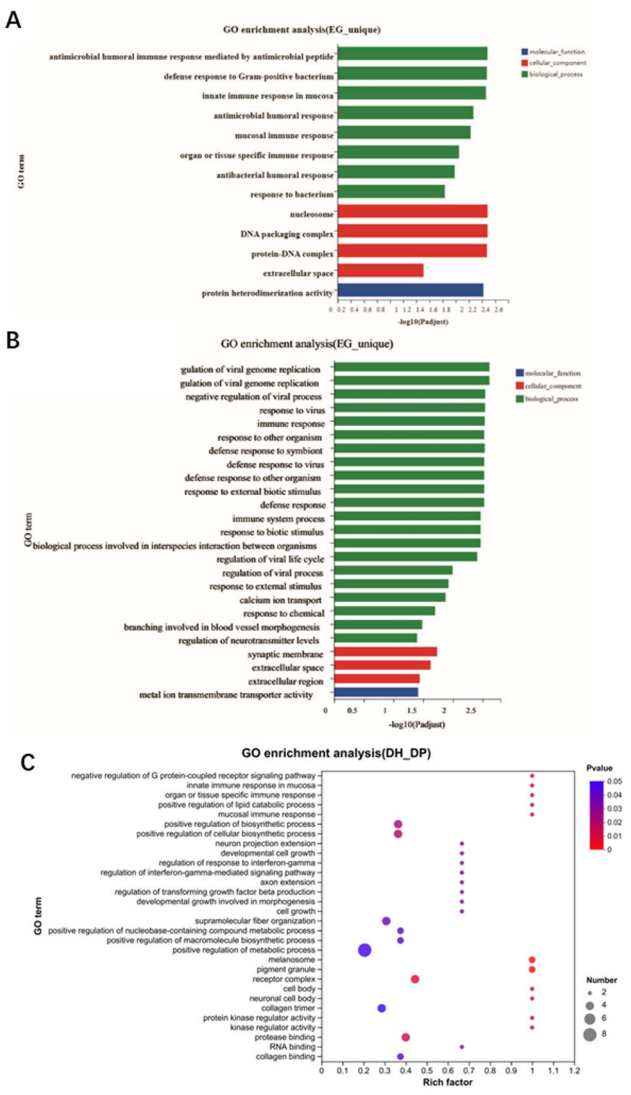

Fig. 6 Significant GO terms of the DEGs and DEPs unique to the Z-EG vs. X-EG group. GO terms with $p < 0.05$ were considered significant. **A** GO enrichment results of DEGs from Lancang samples. **B** GO enrichment results of DEGs from Mangshi samples. **C** GO enrichment results of M-SDPs

immunity (Fig. 6A, B). Consistently, the proteomic data from Mangshi samples also revealed enrichment in key terms such as "innate immune response in mucosa" and "regulation of interferon-gamma-mediated signaling pathway," aligning well with the transcriptomic results. The enrichment results from KEGG pathways further support the preceding statement. These findings suggest that differences in mucosal and innate immune pathways represent a key factor underlying the distinct resistance to piroplasmosis between Yunnan humped cattle and Simmental cattle. Previous studies have demonstrated that both mucosal immunity and innate immunity play crucial roles in combating parasites [43]. Innate immunity serves as the host's most primitive defense mechanism, typically causing minimal damage [44]. These findings are consistent with the physiological function of the mucosa as the first line of defense against pathogens in ruminants [45]. Additionally, the enrichment of IgA production, NK cell-mediated cytotoxicity, and B cell receptor signaling pathways indicates that during the infection process, the two cattle breeds exhibit certain differences in their adaptive immune responses. Notably, the number of differentially expressed proteins identified in plasma was relatively limited. This likely reflects the asymptomatic carrier status of infected animals, in which host systemic proteomic responses are subtle, as well as the inherent dominance of high-abundance proteins in plasma samples. Thus, the observed DEP numbers may reflect biological characteristics.

Key genes and protein biomarkers associated with resistance to piroplasmosis in Yunnan humped cattle

Through integrative analysis, we identified several key candidate genes and proteins associated with piroplasmosis resistance in Yunnan humped cattle. Hub genes such as *CCL4*, *CCL5*, and *IFNB1* encode cytokines that are essential for immune cell recruitment, activation of inflammatory responses, and defense against viral and parasitic infections [46–51]. In addition, *SRC* [52] and *TNFSF11* [53] are involved in immune regulation and signal transduction. Notably, the major histocompatibility complex (MHC) genes *BOLA* (class I) [54] and *BOLA-DRB3* (class II) [55] play critical roles in antigen presentation. These molecules are involved in antigen presentation and pathogen recognition, and previous studies have suggested that their polymorphisms may influence resistance or susceptibility to infectious diseases [56]. Among proteins, HPX and APOA4 were identified as central nodes in the PPI network, with HPX showing higher expression in Yunnan humped cattle. Studies indicate that HPX is protective in severe malaria caused by *Plasmodium vivax* as part of an endogenous protective mechanism [57], and HPX has also been associated with protective immunity in sheep against gastrointestinal nematode infection [58]. High expression of HPX protein in Yunnan humped cattle may indicate that they possess more robust mechanisms to counteract collateral damage caused by infections, thereby protecting their own tissues.

The identification of immune pathways and biomarkers that differ between Yunnan humped and Simmental cattle may reflect long-term interactions between hosts and parasites that have shaped immune-related traits. Yunnan humped cattle have long been exposed to high parasite pressure in tropical and subtropical regions, which may be associated with differences in mucosal and innate immune response. In contrast, Simmental cattle, as an introduced breed, may exhibit distinct immune response profiles under similar environmental conditions. These

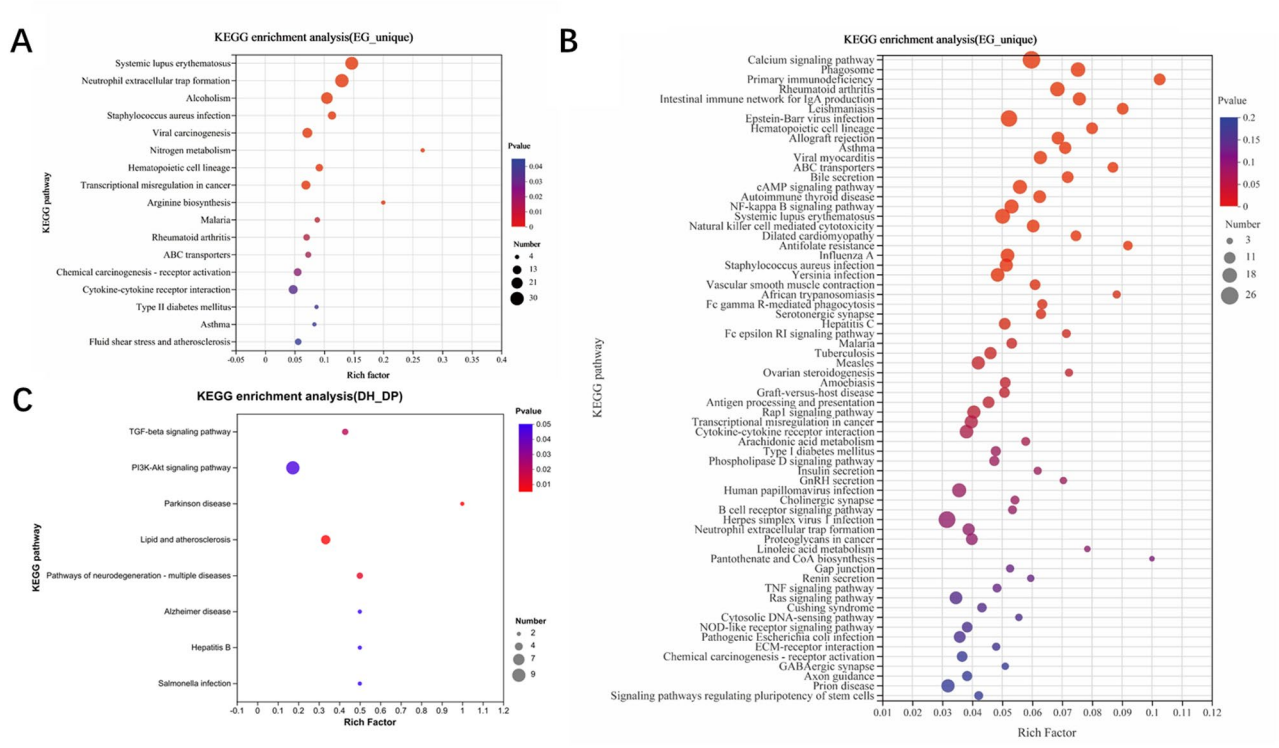

Fig. 7 Significant KEGG pathways of DEGs and DEPs unique to the Z-EG vs. X-EG group. KEGG pathways with $p < 0.05$ were considered significant. **A** KEGG enrichment results of DEGs from Lancang samples. **B** KEGG enrichment results of DEGs from Mangshi samples. **C** KEGG enrichment results of M-SDPs

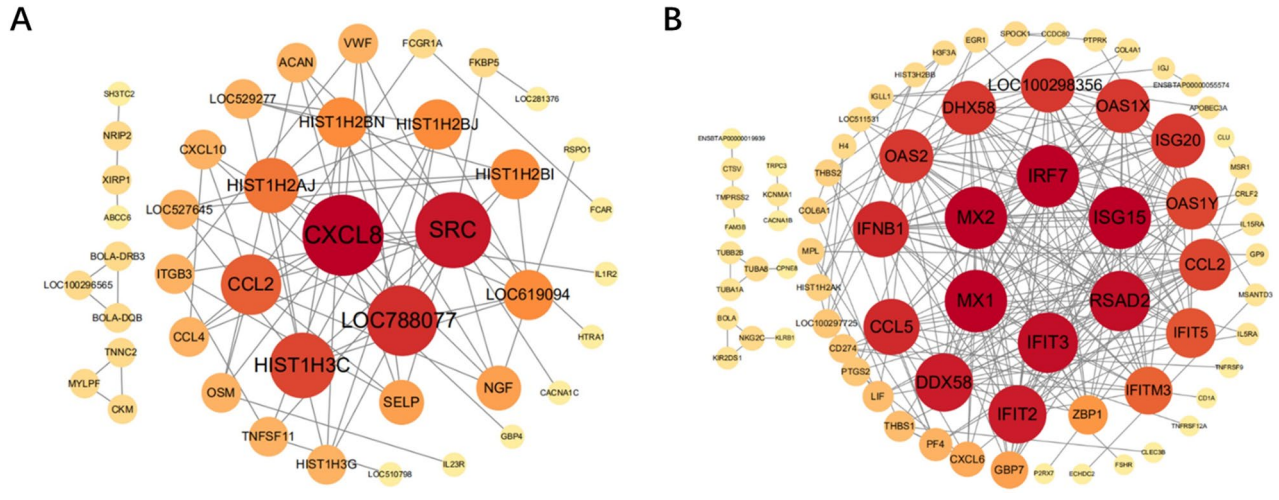

Fig. 8 PPI analysis of selected DEGs using the STRING database. Interactions with confidence score > 0.4 were retained. Node color indicates node degree, with redder colors representing higher degrees. **A** PPI network of selected genes from Lancang samples. **B** PPI network of selected genes from Mangshi samples

findings support the hypothesis that indigenous cattle breeds possess unique genetic advantages for survival in parasite-rich environments. While these observations are suggestive, further studies under controlled conditions are required to disentangle genetic adaptation from environmental influences.

Despite these advances, several limitations should be acknowledged. First of all, samples were collected from two geographically distinct regions with markedly different infection prevalences. Regional differences may reflect a complex combination of ecological and management factors; therefore, regional effects should be interpreted as composite environmental contexts. Importantly, our analyses were performed separately within each region, and biological interpretations focused on immune pathways and candidate

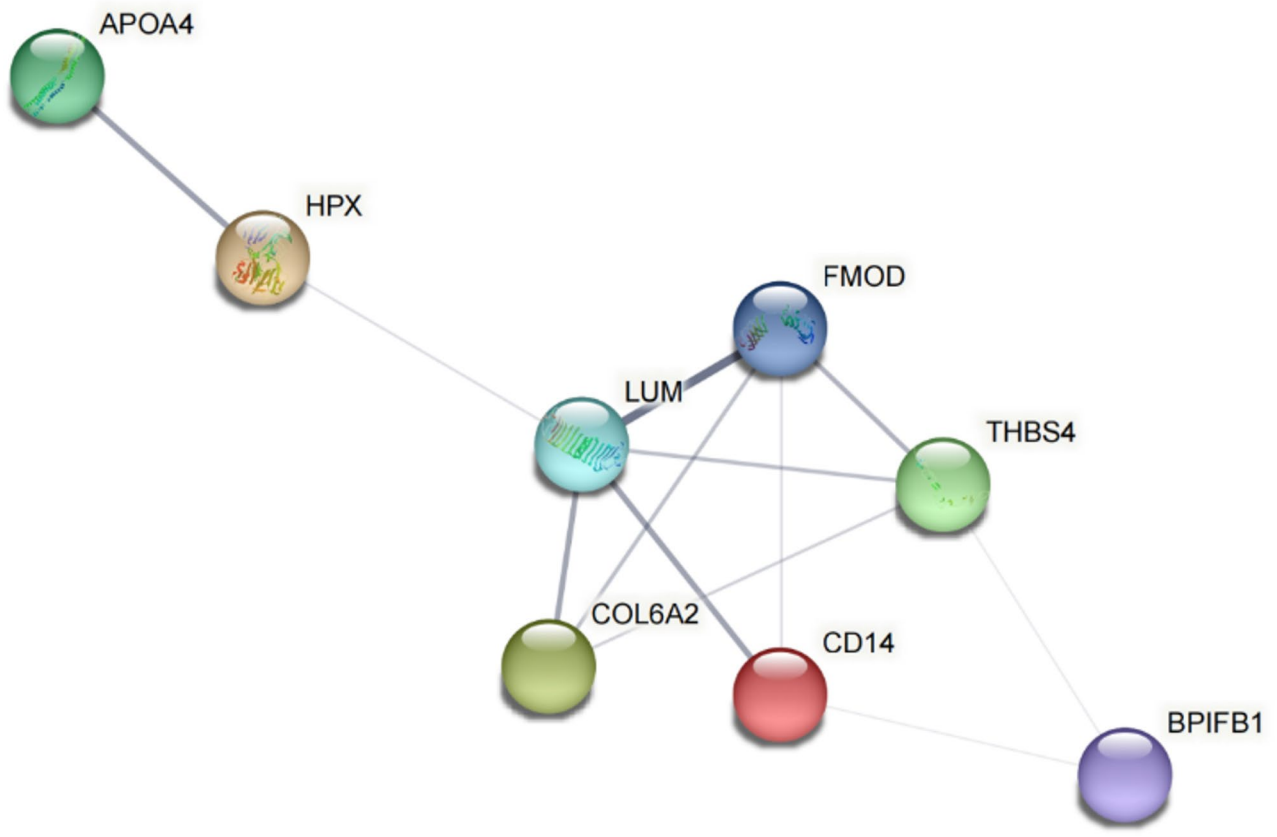

Fig. 9 PPI analysis of selected DEPs using the STRING database. Interactions with a confidence score > 0.4 were retained. The thickness of the lines between nodes is positively correlated with the strength of protein-protein interactions

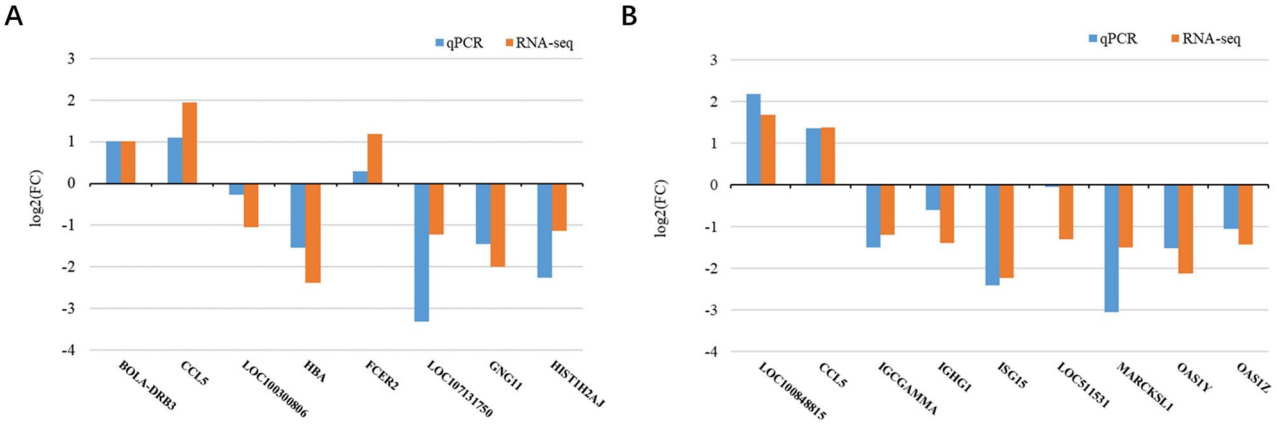

Fig. 10 Comparison of RT-qPCR and RNA-seq results. RT-qPCR data were normalized, and log2 fold changes were used to compare expression trends between RT-qPCR and RNA-seq. **A** The result of genes from Lancang samples. **B** The result of genes from Mangshi samples. Expression trends were consistent with RNA-seq results

molecules that showed consistent expression trends across regions. Nevertheless, future studies incorporating controlled infection models or detailed environmental covariates will be necessary to disentangle host genetic effects from environmental confounders. Second, unequal sample sizes among groups, resulting from natural infection prevalence, may limit statistical power and introduce bias. Accordingly, the conclusions of this study should be interpreted cautiously and primarily as exploratory associations. Because all samples were collected under field conditions, it was impossible to control the infection time, dose, and parasite strain, and functional validation experiments were not performed. Therefore, the observed molecular differences

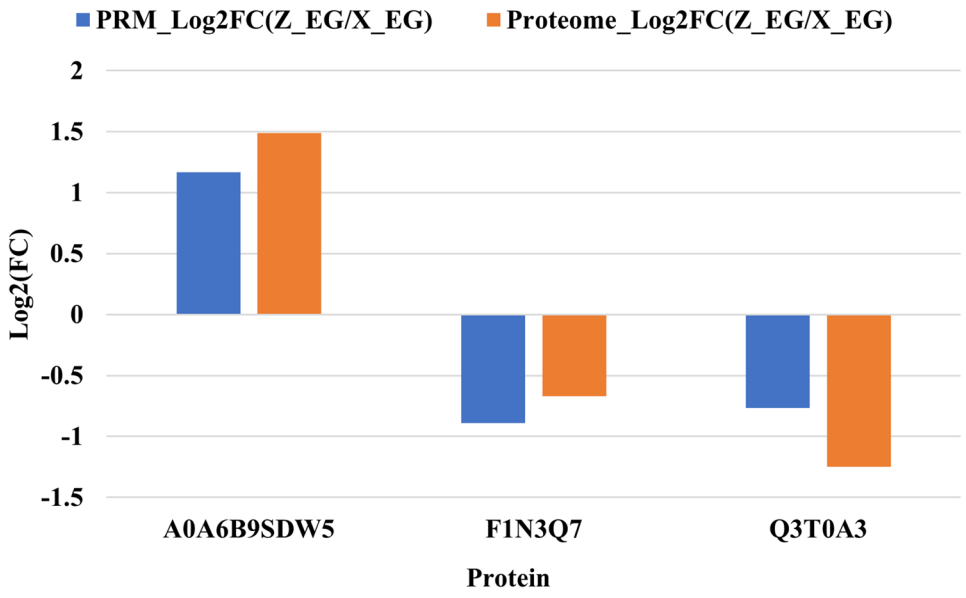

Fig. 11 Comparison of PRM validation and proteomic results in Mangshi samples. Selected DEPs were validated using PRM. Each bar represents one independent DEP. Proteins showing nominal statistical significance ($p < 0.05$, Student's t-test) were included. PRM results showed consistent expression trends with proteomic data

should be interpreted as associations under natural infection conditions rather than direct causal effects. Moreover, the candidate genes and proteins identified in this study should be regarded as promising targets for future investigation rather than definitive determinants of resistance. We also acknowledge that although PCR-based detection provides high sensitivity, false negatives cannot be completely excluded in field-collected samples, and this limitation should be considered when interpreting the infection status and downstream analyses. Future studies incorporating controlled infection experiments, functional validation assays, larger sample sizes, and isotope-labeled standards will be necessary to rigorously confirm the roles of these candidates and to elucidate their underlying mechanisms. Collectively, our findings provide a valuable resource and a foundation for future research aimed at improving disease resistance in cattle through genetic and immunological approaches.

Conclusions

In summary, this study employs integrated multi-omics analysis to investigate breed-specific responses to piroplasm infection across different regions of Yunnan Province. Our results indicate that cattle breed–specific transcriptional and proteomic responses to infection are associated with regional and environmental contexts, suggesting that both genetic background and local conditions may contribute to shaping host immune responses. Yunnan humped cattle and Simmental cattle exhibited distinct molecular response patterns during infection, particularly in pathways related to mucosal and innate immunity. Furthermore, we have identified a series of candidate genes and proteins that were consistently more highly expressed in Yunnan humped cattle and are potentially involved in resistance to piroplasmosis. Although functional validation is still required, these candidate molecules provide promising targets for future studies aimed at elucidating resistance mechanisms and may serve as valuable resources for the development of disease-resilient cattle through long-term breeding strategies.

Abbreviations

Z-EG	Zebu experimental group
Z-CG	Zebu control group
X-EG	Simmental experimental group
X-CG	Simmental control group
RNA-seq	RNA sequencing
MS	Mass spectrometry
DDA	Data-dependent acquisition
DIA	Data-independent acquisition
PRM	Parallel reaction monitoring
TPM	Transcripts Per Million
DEG	Differentially expressed gene
DEP	Differentially expressed protein
L-SDP	Lancang specific differential proteins
M-SDP	Mangshi specific differential proteins
PCA	Principal component analysis
GO	Gene ontology
KEGG	Kyoto encyclopedia of genes and genomes
PPI	Protein-protein interaction networks
LUM	Lumican
FMOD	Fibromodulin
APOA4	Apolipoprotein A4
HPX	Hemopexin isoform X1
MHC	Major histocompatibility complex
TGF	Transforming growth factor

Supplementary Information

The online version contains supplementary material available at https://doi.org/10.1186/s12864-026-12897-3.

Additional file 1: Metadata Summary of Lancang and Mangshi samples.xlsx.

Additional file 2: Sequence of the primer pairs used in this experiment.xlsx.

Additional file 3: PCR results of the piroplasm-positive Yunnan humped cattle.tif.

Additional file 4: The cluster heat map of significantly DEGs between and within two breeds from Lancang and Mangshi samples.tif.

Additional file 5: Summary statistics of the sequencing data.xlsx.

Additional file 6: Details of GO terms and KEGG pathways enriched in this experiment.xlsx.

Additional file 7: The key genes related to the differences in piroplasmosis resistance between Yunnan humped cattle and Simmental cattle.xlsx.

Additional file 8: Analysis of important proteins and PRM validation.xlsx.

Acknowledgements
We would like to express our gratitude to Professor Xuehong Liu of Yunnan Agricultural University for his assistance in collecting samples in Lancang. Additionally, we would like to extend our sincere thanks to Researcher Kaixing Qu of Chuxiong Normal University for his great support and assistance during the sampling process. We also extend our thanks to the staff of the Animal Husbandry station in Mangshi, Dehong Prefecture, for their great assistance in the collection of samples in Mangshi. Finally, we would like to acknowledge Lancang Baolai Agricultural and Livestock Industry Co., Ltd. in Lancang County, Puer City, for providing the Lancang samples.

Authors' contributions
YMC: writing—original draft, review & editing, validation, methodology, investigation, formal analysis, software. XNC: writing—original draft, review & editing, validation, methodology, investigation, formal analysis, software. RL: methodology, investigation, formal analysis, resources. CQL: methodology, formal analysis, resources. HX: methodology, supervision, resources, conceptualization. SYC: writing—original draft, review & editing, methodology, supervision, resources, project administration, funding acquisition, conceptualization. All authors read and approved the final manuscript.

Funding
This work was supported by the National Natural Science Foundation of China (32160146), the Top Young Talents Program of Ten Thousand Plan of Yunnan Province (YNWR-QNBJ-2018-024), and the 13th Graduate Research and Innovation Project of Yunnan University (2021Y292).

Data availability
The RNA-seq data generated during the current study have been deposited in the Genome Sequence Archive [59] in National Genomics Data Center [60], China National Center for Bioinformation/Beijing Institute of Genomics, Chinese Academy of Sciences, under accession number CRA028992 (https://ngdc.cncb.ac.cn/gsa/browse/CRA028992). The mass spectrometry proteomics data have been deposited to the ProteomeXchange Consortium via the iProX partner repository [61, 62] with the project ID: PXD076555 (https://proteomecentral.proteomexchange.org/?pxid=PXD076555).

Declarations

Ethics approval and consent to participate
Blood samples were collected by veterinary practitioners with the permission and in the presence of the owners and under permission from the Guide for the Care and Use of Laboratory Animals of Yunnan University. Veterinarians followed standard procedures and relevant national guidelines to ensure appropriate animal care. This study was approved by the Committee on Animal Research and Ethics of Yunnan University (Approval number: ynucae20190011).

Consent for publication
Not applicable.

Competing interests
The authors declare no competing interests.

Received: 4 September 2025 / Accepted: 27 April 2026
Published online: 30 April 2026

References

1. Schnittger L, Yin H, Gubbels MJ, Beyer D, Niemann S, Jongejan F, et al. Phylogeny of sheep and goat Theileria and Babesia parasites. Parasitol Res. 2003;91:398–406.
2. Schnittger L, Yin H, Qi B, Gubbels MJ, Beyer D, Niemann S, et al. Simultaneous detection and differentiation of Theileria and Babesia parasites infecting small ruminants by reverse line blotting. Parasitol Res. 2004;92:189–96.
3. Gou H, Guan G, Liu A, Ma M, Xu Z, Liu Z, et al. A DNA barcode for Piroplasmea. Acta Trop. 2012;124:92–7.
4. Lakew BT, Kheravii SK, Wu SB, Eastwood S, Andrew NR, Jenkins C, et al. Endemic infection of cattle with multiple genotypes of Theileria orientalis on the Northern Tablelands of New South Wales despite limited presence of ticks. Ticks Tick Borne Dis. 2021;12:101645.
5. Youying L, Lan L, Yao P, Danjiao Y, Jianping W, Songming L, et al. Molecular epidemiological investigation and species identification of Theileria infection in yaks in Litang County of Sichuan Province. Anim Husb Veterinary Med. 2021;53:61–6.
6. Ruiqi S, Huercha, Xinli F, Xuejie Z, Min L, Yunwei H, et al. Investigation and analysis of epidemic related factors for equine piroplasma in Zhaosu,Xinjiang. Chin J Veterinary Sci. 2021;41:62–7.
7. Hummler M. The First Steps of Animal Domestication: New archaeological approaches. Antiquity. 2006;80:751–2.
8. Cohen NR, Lobritz MA, Collins JJ. Microbial persistence and the road to drug resistance. Cell Host Microbe. 2013;13:632–42.
9. Jensen K, Paxton E, Waddington D, Talbot R, Darghouth MA, Glass EJ. Differences in the transcriptional responses induced by Theileria annulata infection in bovine monocytes derived from resistant and susceptible cattle breeds. Int J Parasitol. 2008;38:313–25.
10. Trevisi E, Zecconi A, Cogrossi S, Razzuoli E, Grossi P, Amadori M. Strategies for reduced antibiotic usage in dairy cattle farms. Res Vet Sci. 2014;96:229–33.
11. Glass EJ, Jensen K. Resistance and susceptibility to a protozoan parasite of cattle–gene expression differences in macrophages from different breeds of cattle. Vet Immunol Immunopathol. 2007;120:20–30.
12. Marima JK, Nel CL, Marufu MC, Jonsson NN, Dube B, Dzama K. A genetic and immunological comparison of tick-resistance in beef cattle following artificial infestation with Rhipicephalus ticks. Exp Appl Acarol. 2020;80:569–90.
13. Chen SY, Lin BZ, Baig M, Mitra B, Lopes RJ, Santos AM, et al. Zebu cattle are an exclusive legacy of the South Asia Neolithic. Mol Biol Evol. 2010;27:1–6.
14. Yueyun Y, Liming S. Animal Genetic Resources in Yunnan. Yunnan Kunming: Yunnan Science and Technology; 2014.
15. Mattioli RC, Pandey VS, Murray M, Fitzpatrick JL. Immunogenetic influences on tick resistance in African cattle with particular reference to trypanotolerant N'Dama (*Bos taurus*) and trypanosusceptible Gobra zebu (Bos indicus) cattle. Acta Trop. 2000;75:263–77.
16. Franzin AM, Maruyama SR, Garcia GR, Oliveira RP, Ribeiro JM, Bishop R, et al. Immune and biochemical responses in skin differ between bovine hosts genetically susceptible and resistant to the cattle tick Rhipicephalus microplus. Parasit Vectors. 2017;10:51.
17. Jonsson NN, Piper EK, Constantinoiu CC. Host resistance in cattle to infestation with the cattle tick Rhipicephalus microplus. Parasite Immunol. 2014;36:553–9.
18. Bechara GH, Morelli Junior J, Szabo MP. Skin test and tick immune status in susceptible and resistant cattle in Brazil. Ann N Y Acad Sci. 2000;916:570–5.
19. Ndungu SG, Brown CGD, Dolan TT. In vivo comparison of susceptibility between Bos indicus and *Bos taurus* cattle types to Theileria parva infection. Onderstepoort J Vet. 2005;72:13–22.
20. Jonsson NN, Bock RE, Jorgensen WK. Productivity and health effects of anaplasmosis and babesiosis on Bos indicus cattle and their crosses, and

the effects of differing intensity of tick control in Australia. Vet Parasitol. 2008;155:1–9.
21. Yunxia Q, Yongbin L, Weiheng R. RNA-Seq and its applications:a new technology for transcriptomics. Hereditas(Beijing). 2011;33:1191–202.
22. Haynes SE, Majmudar JD, Martin BR. DIA-SIFT: A precursor and product ion filter for accurate stable isotope data-independent acquisition proteomics. Anal Chem. 2018;90:8722–6.
23. Cho KC, Clark DJ, Schnaubelt M, Teo GC, Leprevost FDV, Bocik W, et al. Deep proteomics using two dimensional data independent acquisition mass spectrometry. Anal Chem. 2020;92:4217–25.
24. Michalski A, Cox J, Mann M. More than 100,000 detectable peptide species elute in single shotgun proteomics runs but the majority is inaccessible to data-dependent LC-MS/MS. J Proteome Res. 2011;10:1785–93.
25. Zhang D, Li Y, Liang M, Liang Y, Tian J, He Q, et al. LC-MS/MS based metabolomics and proteomics reveal candidate biomarkers and molecular mechanism of early IgA nephropathy. Clin Proteom. 2022;19:51.
26. Han S, Zhang J, Sun Y, Liu L, Guo L, Zhao C et al. The plasma DIA-Based quantitative proteomics reveals the pathogenic pathways and new biomarkers in cervical cancer and high grade squamous intraepithelial lesion. J Clin Med. 2022;11.
27. Tognetti M, Sklodowski K, Muller S, Kamber D, Muntel J, Bruderer R, et al. Biomarker candidates for tumors identified from deep-profiled plasma stem predominantly from the low abundant area. J Proteome Res. 2022;21:1718–35.
28. Jia X, Zhai TY, Zhang JA. Circulating exosome involves in the pathogenesis of autoimmune thyroid diseases through immunomodulatory proteins. Front Immunol. 2021;12.
29. Caiqin S. Development of the PCR for detection of piroplasms infective to cattle and sheep in Hoemaphysalis qinghaiensis and its application. Master's thesis. Gansu Agricultural University; 2005.
30. Xueying S, Zhihai H, Guozhang F, Mingguo Y, Yun Z, Jiafu J, et al. Molecular epidemiological investigation of piroplasma infection in cattle and sheep in Tengchong, Yunnan Province. Anim Husb Veterinary Med. 2020;52:61–8.
31. Modi A, Vai S, Caramelli D, Lari M. The Illumina Sequencing Protocol and the NovaSeq 6000 System. Methods Mol Biol. 2021;2242:15–42.
32. Ewels P, Magnusson M, Lundin S, Käller M. MultiQC: summarize analysis results for multiple tools and samples in a single report. Bioinformatics. 2016;32:3047–8.
33. Kim D, Paggi JM, Park C, Bennett C, Salzberg SL. Graph-based genome alignment and genotyping with HISAT2 and HISAT-genotype. Nat Biotechnol. 2019;37:907–.
34. Love MI, Huber W, Anders S. Moderated estimation of fold change and dispersion for RNA-seq data with DESeq2. Genome Biol 2014;15.
35. Orsburn BC. Proteome discoverer-A community enhanced data processing suite for protein informatics. Proteomes. 2021;9.
36. Muller F, Rappsilber J. A protocol for studying structural dynamics of proteins by quantitative crosslinking mass spectrometry and data-independent acquisition. J Proteom. 2020;218.
37. Sang J, Wang Z, Li M, Cao J, Niu G, Xia L, et al. ICG: a wiki-driven knowledgebase of internal control genes for RT-qPCR normalization. Nucleic Acids Res. 2018;46:D121–6.
38. Peterson AC, Russell JD, Bailey DJ, Westphall MS, Coon JJ. Parallel Reaction Monitoring for High Resolution and High Mass Accuracy Quantitative, Targeted Proteomics. Mol Cell Proteom. 2012;11:1475–88.
39. Ronsein GE, Pamir N, von Haller PD, Kim DS, Oda MN, Jarvik GP, et al. Parallel reaction monitoring (PRM) and selected reaction monitoring (SRM) exhibit comparable linearity, dynamic range and precision for targeted quantitative HDL proteomics. J Proteom. 2015;113:388–99.
40. MacLean B, Tomazela DM, Shulman N, Chambers M, Finney GL, Frewen B, et al. Skyline: an open source document editor for creating and analyzing targeted proteomics experiments. Bioinformatics. 2010;26:966–8.
41. Hansen PJ. Physiological and cellular adaptations of zebu cattle to thermal stress. Anim Reprod Sci. 2004;82–83:349–60.
42. Vijayakumar P, Singaravadivelan A, Mishra A, Jagadeesan K, Bakyaraj S, Suresh R, et al. Whole-genome comparative analysis reveals genetic mechanisms of disease resistance and heat tolerance of tropical Bos indicus cattle breeds. Genome. 2022;65:241–54.
43. Rittipornlertrak A, Nambooppha B, Muenthaisong A, Apinda N, Koonyosying P, Srisawat W, et al. Immunization of cattle with recombinant structural ectodomains I and II of babesia bovis apical membrane antigen 1 [BbAMA-1(I/II)] induces strong Th1 immune response. Front Vet Sci. 2022;9:917389.
44. Sun LZ, Wang XW, Saredy J, Yuan ZY, Yang XF, Wang H. Innate-adaptive immunity interplay and redox regulation in immune response. Redox Biol. 2020;37.
45. Chase C, Kaushik RS. Mucosal Immune System of Cattle: All Immune Responses Begin Here. Vet Clin North Am Food Anim Pract. 2019;35:431–51.
46. Shao W, Tang J, Song W, Wang C, Li Y, Wilson CM, et al. CCL3L1 and CCL4L1: variable gene copy number in adolescents with and without human immunodeficiency virus type 1 (HIV-1) infection. Genes Immun. 2007;8:224–31.
47. Chen R, Ma L, Jiang C, Zhang S. Expression and potential role of CCL4 in CD8 + T cells in NSCLC. Clin Transl Oncol. 2022;24:2420–31.
48. Sun BM, Lei Y, Cao ZJ, Zhou YC, Sun Y, Wu Y, et al. TroCCL4, a CC chemokine of Trachinotus ovatus, is involved in the antimicrobial immune response. Fish Shellfish Immunol. 2019;86:525–35.
49. Esche C, Stellato C, Beck LA, Chemokines. Key players in innate and adaptive immunity. J Invest Dermatol. 2005;125:615–28.
50. Schlechter BL, Stebbing J. CCR5 and CCL5 in metastatic colorectal cancer. J Immunother Cancer. 2024;12.
51. Witt KC, Dziulko A, An J, Pekovic F, Cheng AX, Liu GY, et al. SP140-RESIST pathway regulates interferon mRNA stability and antiviral immunity. Nature. 2025;643:1372–80.
52. Pare G, Vitry J, Merchant ML, Vaillancourt M, Murru A, Shen Y, et al. The Inhibitory Receptor CLEC12A Regulates PI3K-Akt Signaling to Inhibit Neutrophil Activation and Cytokine Release. Front Immunol. 2021;12:650808.
53. Anderson DM, Maraskovsky E, Billingsley WL, Dougall WC, Tometsko ME, Roux ER, et al. A homologue of the TNF receptor and its ligand enhance T-cell growth and dendritic-cell function. Nature. 1997;390:175–9.
54. Ellis SA, Holmes EC, Staines KA, Smith KB, Stear MJ, McKeever DJ, et al. Variation in the number of expressed MHC genes in different cattle class I haplotypes. Immunogenetics. 1999;50:319–28.
55. Valenzano MN, Caffaro ME, Lia VV, Poli M, Wilkowsky SE. Diversity of the BoLA-DRB3 gene in cattle breeds from tropical and subtropical regions of Argentina. Trop Anim Health Prod. 2021;54:23.
56. Glass EJ, Crutchley S, Jensen K. Living with the enemy or uninvited guests: Functional genomics approaches to investigating host resistance or tolerance traits to a protozoan parasite, Theileria annulata, in cattle. Vet Immunol Immunop. 2012;148:178–89.
57. Elphinstone RE, Conroy AL, Hawkes M, Hermann L, Namasopo S, Warren HS, et al. Alterations in systemic extracellular heme and hemopexin are associated with adverse clinical outcomes in Ugandan Children with severe Malaria. J Infect Dis. 2016;214:1268–75.
58. Knight JS, Baird DB, Hein WR, Pernthaner A. The gastrointestinal nematode Trichostrongylus colubriformis down-regulates immune gene expression in migratory cells in afferent lymph. Bmc Immunol. 2010;11.
59. Chen TT, Chen X, Zhang SS, Zhu JW, Tang BX, Wang AK, et al. Genom Proteom Bioinf. 2021;19:578–83. The Genome Sequence Archive Family: Toward Explosive Data Growth and Diverse Data Types.
60. Bao YM, Zhang Z, Zhao WM, Xiao JF, Song SH, He SM, et al. Database Resources of the National Genomics Data Center, China National Center for Bioinformation in 2025. Nucleic Acids Res. 2024;53:D30–44.
61. Ma J, Chen T, Wu SF, Yang CY, Bai MZ, Shu KX, et al. iProX: an integrated proteome resource. Nucleic Acids Res. 2019;47:D1211–7.
62. Chen T, Ma J, Liu Y, Chen ZG, Xiao N, Lu YT, et al. iProX in 2021: connecting proteomics data sharing with big data. Nucleic Acids Res. 2022;50:D1522–7.

Publisher's Note